# Screen Printable Epoxy/$BaTiO_3$ Embedded Capacitor Pastes with High Dielectric Constant for Organic Substrate Applications

**Kyung-Woon Jang, Kyung-Wook Paik**

*Department of Materials Science and Engineering, KAIST, 373-1, Guseong-Dong, Yuseong-Gu, Daejeon 305-701, Republic of Korea*

Received 7 October 2007; accepted 1 April 2008
DOI 10.1002/app.28515
Published online 10 July 2008 in Wiley InterScience (www.interscience.wiley.com).

**ABSTRACT:** In this article, embedded capacitor pastes (ECPs) with various $BaTiO_3$ (BTO) powder contents were formulated and screen-printed on PCBs to fabricate capacitors. The material properties of the ECPs that included their rheology, curing behavior, and dielectric constant were investigated. Embedded capacitors were fabricated for reliability tests related to the thermal cycling and high temperature and humidity potential of optimized ECPs. Additionally, changes in the dielectric properties were discussed. ECPs were formulated with various powder contents from 0 to 70 vol %. ECP resin was cured at temperatures ranging from 130 to 220°C. All ECPs had the viscosities below 30 Pa · s at a shear rate of 100 $s^{-1}$ to be easily screen-printable. The dielectric constant of the cured ECPs increased to 60 at 70 vol %, and the dielectric loss was approximately 0.023 for all ECPs regardless of BTO volume content. For the reliability test, ECPs with 50, 60, and 70 vol % BTO powder contents were selected and embedded capacitors were fabricated. After a thermal cycling test with a temperature range from −55 to 125°C for 1000 cycles, capacitance decreased by approximately 5 ~ 10%, but the dielectric loss did not change. After a 85°C/85RH% test for 1000 h, the capacitance and dielectric loss increased by nearly 20%. Cyanoresin (CRS) was used to form the high dielectric polymer/ceramic composite material. The newly formulated resin system had a dielectric constant that is double that of a conventional epoxy resin system. Additionally, the dielectric constant of the polymer/ceramic composite material increased 50% at 50 vol %. © 2008 Wiley Periodicals, Inc. J Appl Polym Sci 110: 798–807, 2008

**Key words:** embedded capacitor; screen printing; polymer/ceramic composite; dielectric constant; reliability

## INTRODUCTION

Electronic systems are composed of active components, such as ICs and passive components. Passive components are attracting increasing levels of interest, as the number of passive components is steadily growing as the electronics industry progresses toward higher functionality.[1] For example, the ratio of the passive to active components in mobile cellular phones is greater than 20.[2] Currently, most the passive components are surface-mounted and have discrete forms. Therefore, they take up a large area of the substrates and have lower electrical performance because of their longer interconnection length. To solve these problems, embedded passive technology, which incorporates passive components into an inner layer within multi-layer substrates, has been actively investigated.

Among the passive components, capacitors have been most widely studied, as they are used in various areas. Examples include decoupling, by-passing, filtering, and timing capacitors. In particular, great interest has been concentrated on replacing discrete decoupling capacitors, which are used for simultaneous switching noise suppression, into a form of embedded capacitor. Embedded decoupling capacitors show better electrical performance because of the reduced level of parasitic inductance.

Embedded capacitor materials require a high dielectric constant, low capacitance tolerance, good processability, and a low cost. Thus far, however, no single material has met these requirements. For example, thin film capacitor materials formed by vacuum deposition have the advantage of comparatively high capacitance, whereas they have drawbacks of a high processing temperature and a high cost.

Polymer/ceramic composites, which are polymers filled with ceramic powders, are among the most promising materials for embedded capacitors.[3–5] They have the high dielectric constant of ceramic powders and the good processability of polymers, resulting in a process with lower temperatures and a lower cost. A spin-coating method has been extensively used for the deposition of polymer/ceramic

*Correspondence to:* K.-W. Jang (amiha@kaist.ac.kr).

Journal of Applied Polymer Science, Vol. 110, 798–807 (2008)
© 2008 Wiley Periodicals, Inc.

composites,[5–7] as the spin-coating method has the major advantage of thinner film fabrication, which leads to higher capacitance. However, the spin-coating method has major technical difficulties which must be addressed. The first issue is the associated high level of material waste, and the second is the nonuniform thickness control of the films, which results in nonuniform electrical properties for capacitors over a large area. Recently, a tape-casting method was suggested to fabricate polymer/ceramic composite films with a uniform thickness.[8] The two aforementioned methods are limited in terms of their inability to form a capacitor layer in a local area. This is undesirable, as parasitic inductance occurs if a dielectric layer is formed over the entire area on printed circuit boards (PCBs). It was for this reason that the screen-printable epoxy/BTO composite embedded capacitor pastes (ECPs) are designed in this study. ECPs have an advantage that capacitors can be formed locally for a desired part via a mask pattern using a screen-printing method. However, ECPs also have the problem of a high tolerance, as the edge of a screen-printed layer is generally thicker than its center because of the surface tension of mask.

In this work, screen-printable ECPs with various BTO powder contents were fabricated, and the material properties of the ECPs of the curing behavior, viscosity, and dielectric constant were investigated. Embedded capacitors were fabricated for thermal cycling and high temperature/humidity reliability tests. The changes in the dielectric constant during the reliability tests were discussed. In addition, a novel high dielectric constant-resin system containing cyanoresin was formulated.

## EXPERIMENTAL

### Materials

#### ECP resin system

ECP essentially consists of a liquid Bisphenol-A type epoxy, a thermoplastic polymer (T/P), solvents, BTO powder, and a curing agent. Bisphenol-A type epoxy is utilized for high temperature stability after curing. Vinyl-type thermoplastic polymer with a high molecular weight (~ 170,000) was used for screen-printability and resistance to moisture absorption. The solvent was used to dissolve T/P resin and reduce the viscosity of the ECPs. As a curing agent, dicyandiamide (DICY: $NH_2NHCNHCN$) was used. DICY is a latent curing agent used for high temperature curing; curing reaction does not proceed with this agent at room temperature.[9] This enables easier handling, as the viscosity of the ECPs does not change during the fabrication process and screen printing process. In addition, the screen-printed thick film layer can be kept at the B-stage after the drying process.

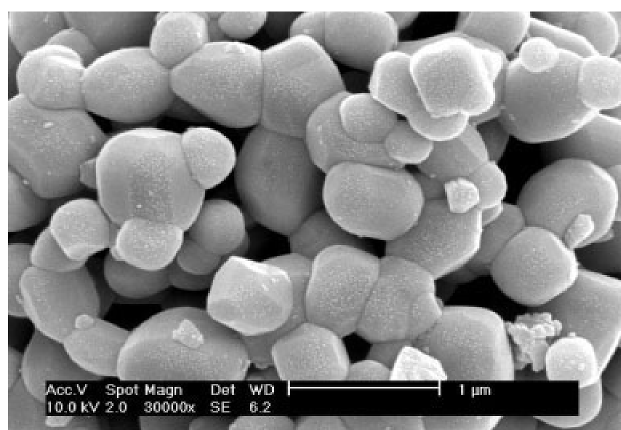


**Figure 1** SEM image of the BTO powder.

#### BTO powder

BTO is widely known to be a high dielectric constant material. The dielectric constant of bulk BTO is affected by its grain size at room temperature. Its dielectric constant increases to the maximum with a decrease in the grain size to approximately 0.9 μm, whereas it decreases further when its grain size is below 0.9 μm. The dielectric constant of bulk BTO strongly depends on the crystal structure of BTO. BTO powder has similar characteristics to the dielectric constant of bulk BTO. At room temperature, tetragonality decreases as the particle size decreases slowly to 0.3 μm. The tetragonality of BTO powder with a particle size less than 0.3 μm rapidly decreases, eventually disappearing when reaching approximately 0.1 μm. This implies that structural changes to the cubic or pseudocubic structure.[10,11] Therefore, it can be expected that BTO powder will have the maximum dielectric constant at approximately 0.9 μm, and this has been verified.[8] Therefore, BTO powder with average size of 0.9 μm was chosen for the purposes of this study. BTO powder was purchased from SAKAI Chemical Industry Co., (Osaka, Japan). The BTO powder was hydrothermally produced and its purity was above 99.9%. The specific surface area was $2.7 \pm 0.3\ m^2/g$. Figure 1 shows a SEM image of the BTO powder used in this study.

### Fabrication process

#### Formation of ECPs

The fabrication processes for the ECPs can be described as follows: (1) Liquid epoxy resin, thermoplastic resin, a dispersant, and a coupling agent were mixed in a rotational mixer for 3 min. (2) BTO

powder was added to the mixture and mixed in a rotational mixer for 5 min. (3) To break agglomerates of the BTO powder, the resin system underwent a three-roll mill mixing process three times. (4) After adding the curing agent, the resin system underwent the three-roll mill mixing process an additional time.

ECPs should be kept in a freezer to prevent curing. Whenever ECPs are used for experiments here, they were remixed in the rotational mixer for 60 to 90 s after melting.

## Curing and rheological characterization

The curing property of the ECP resin was investigated using DSC (Differential Scanning Calorimetry). In a dynamic scan mode, the ECP resin was heated from 50 to 300°C at a heating rate of 10°C/min in a nitrogen atmosphere. To measure the cure times of the ECP resin, an isothermal scan was performed at various temperatures.

The rheological properties of the ECPs were investigated using a plate-and-plate rotational rheometer. ECPs with various powder contents were sheared between a cone and the plate for 2 min as the shear rate increased from 0 $s^{-1}$ to 100 $s^{-1}$. After the shear rate reached its maximum value, it was decreased again from 100 $s^{-1}$ to 0 $s^{-1}$ for 2 min.

## Capacitor fabrication and measurement

Using the ECPs, metal–insulator–metal structures were fabricated. First, ECPs were printed on PCBs using a screen printer. Conditions for the screen printing are as follows: (1) squeegee hardness: 90 durometer, (2) squeegee angle: 45°, (3) printing mask mesh: 250 mesh, (4) mask emulsion thickness: 10 μm, (5) snap-off distance: 1 mm, and (6) printing speed: 30 mm/s. Second, the ECPs screen-printed on PCBs were dried on a hot-plate at 80°C for 30 min

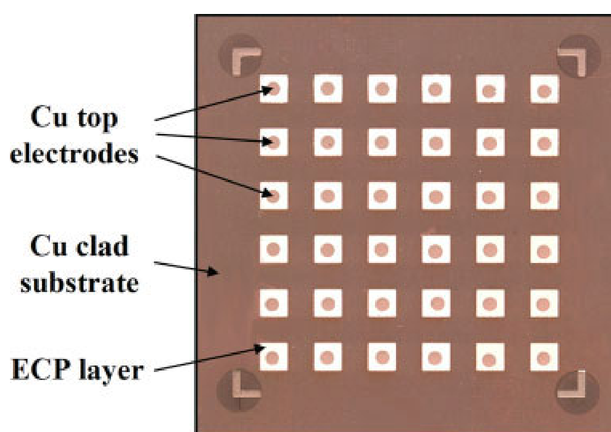


**Figure 2** Photographic image of a fabricated capacitor sample. [Color figure can be viewed in the online issue, which is available at www.interscience.wiley.com.]

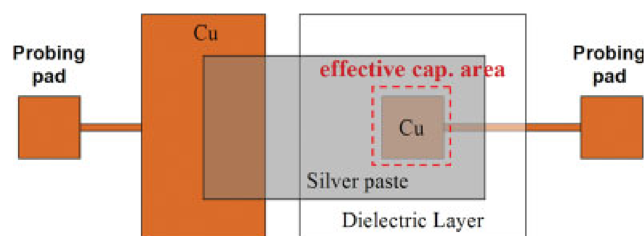


**Figure 3** Schematic diagram of the circuit designed for embedded capacitor. [Color figure can be viewed in the online issue, which is available at www.interscience.wiley.com.]

to remove the solvent. After the drying process, the ECPs were cured in a laminator at a pressure of 50 psi. The temperature profile for the curing was 80°C/30 min and 180°C/60 min. ECPs were kept at 80°C for 30 min to give ECPs fluidity at the B-stage. After the curing process, metal (Cu) top electrodes were deposited by a sputtering method using a shadow mask. The area of the top electrode was 3.14 $mm^2$. Figure 2 shows a photographic image of a fabricated capacitor sample.

The thickness of ECPs was measured using surface profiler (α-step 500), and their capacitance and dielectric loss were measured at 100 kHz using a HP 4284A LCR meter. The dielectric constant was calculated from the measured thickness and the capacitance.

## Embedded capacitor and reliability test

To characterize material reliability of the ECPs, embedded capacitors were fabricated. Figure 3 shows a schematic diagram of the circuit designed for the embedded capacitors, and Figure 4 illustrates the fabrication process of the embedded capacitors. First, ECPs were screen-printed on patterned bottom electrodes. The area of the screen-printed ECP was larger than that of the bottom electrode to use a relatively flat part of the screen-printed layer as an effective capacitor area. This was done because the edge of a screen-printed layer is generally thicker than its center due to the surface tension of the mask. Second, silver paste was screen-printed onto a cured ECP layer. As shown in Figure 3, the silver paste was connected to the other electrode to measure the capacitance. The capacitance can be measured at the pads on the backside of the sample. Final, capacitors were embedded using a prepreg bonding process.

For the reliability tests, three types of ECPs containing 50, 60, and 70 vol % powder were selected as the capacitor materials. A thermal cycling test (−55°C/15 min ~ 125°C/15 min) and a high temperature/high humidity test (85°C/85RH%) were performed for 1000 cycles and 1000 h, respectively.

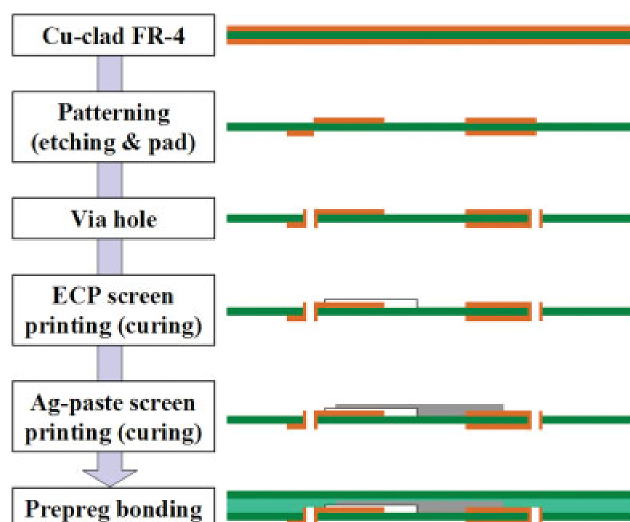


**Figure 4** Fabrication process for the demonstration of embedded capacitor. [Color figure can be viewed in the online issue, which is available at www.interscience.wiley.com.]

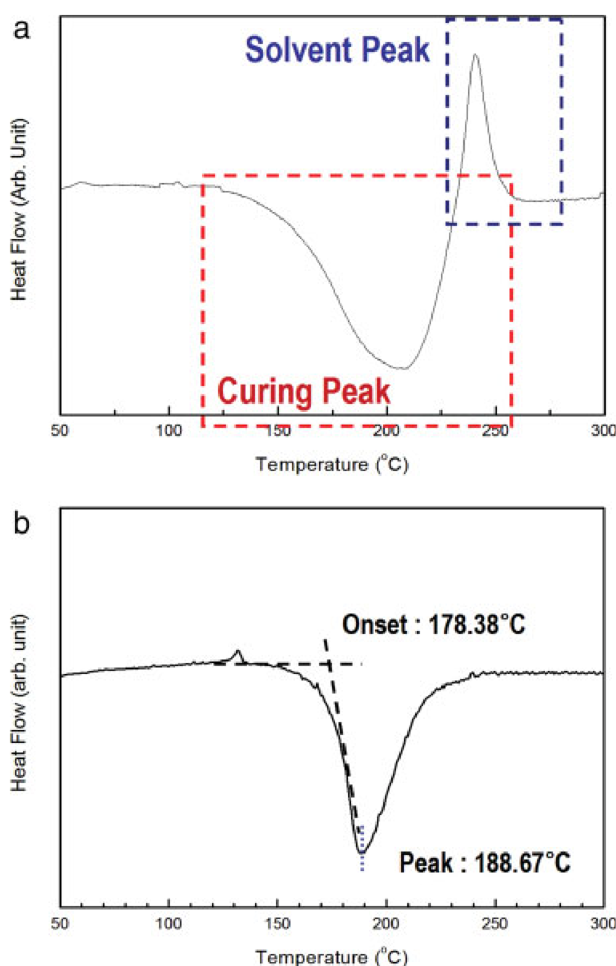


**Figure 5** Heat flow changes of the ECP resin (a) before the drying process and (b) after the drying process as a function of temperature. [Color figure can be viewed in the online issue, which is available at www.interscience.wiley.com.]

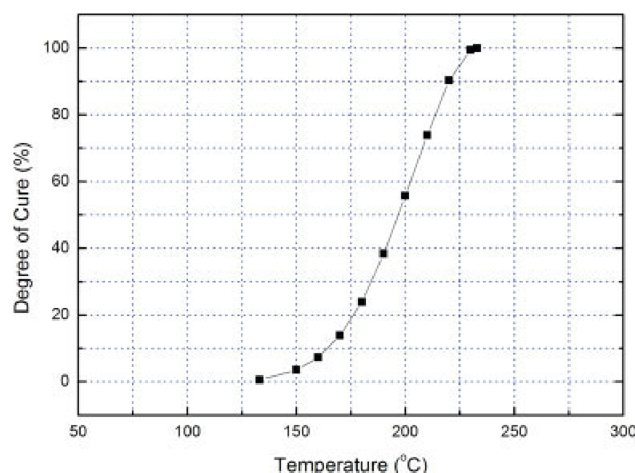


**Figure 6** Degree of cure of the ECP resin as a function of temperature. [Color figure can be viewed in the online issue, which is available at www.interscience.wiley.com.]

## RESULTS AND DISCUSSION

### Curing property

Figure 5 shows the heat flow changes of the ECP resin with no powder in dynamic scan modes. Figure 5(a) shows the heat flow changes of the ECP resin before the drying process, and Figure 5(b) shows the heat flow changes of ECP resin after a drying process of 80°C for 20 min. Comparing the two figures, Figure 5(a) shows the solvent vaporization peak at approximately 220°C. However, Figure 5(b) shows no solvent vaporization peak. From this result, the drying condition was determined to be 80°C for 30 min to guarantee a sufficient drying time.

Figure 6 shows the degree of cure calculated from the resin in Figure 5(b) as a function of temperature. It was found that the curing of the ECP resin begins at 130°C and ends at 220°C. The endothermic peak at about 230°C is a solvent-vaporization peak. Figure 7 shows the heat flow changes of the ECP resin at various temperatures. As shown in Figure 7, an exothermic reaction took place as the scanning time increased, and the heat flow decreased again after curing. This was most likely because of a mass reduction via solvent vaporization. The end-point of curing is the maximum point of the heat flow. The X marks in Figure 7 indicate the maximum points of the heat flow curves. Cure times at various temperatures are summarized in Table I. From the above results, the drying condition and curing condition were set to 100°C for 30 min and 180°C for 60 min, respectively.

### Rheology

Figure 8 shows the viscosity curves of the ECPs as a function of shear rate. The viscosities of the ECPs gradually decreased as the powder contents

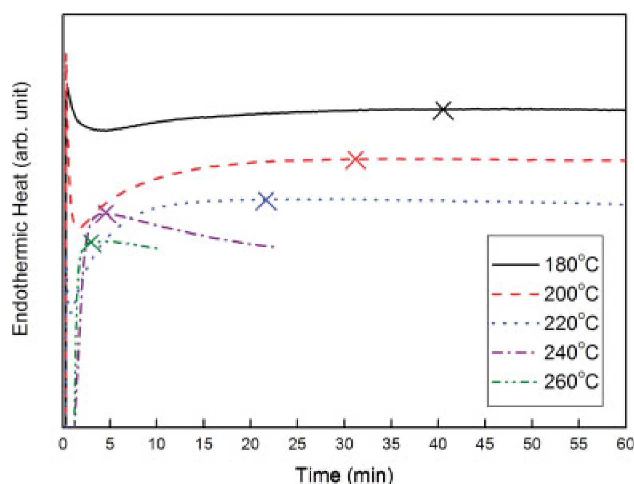


Figure 7 Heat flow changes of the ECP resin at various temperatures in isothermal modes. [Color figure can be viewed in the online issue, which is available at www.interscience.wiley.com.]

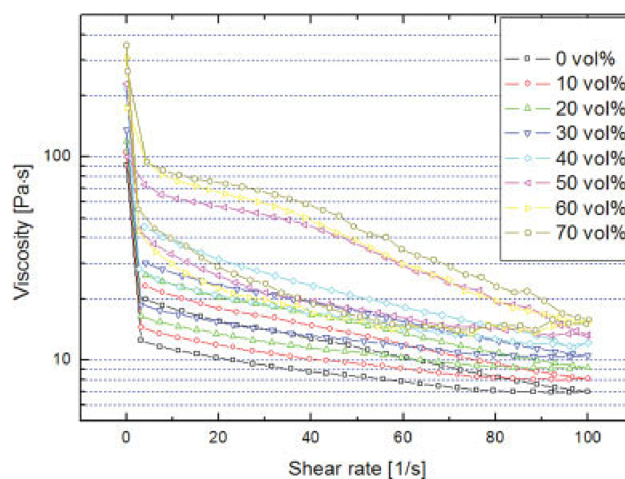


Figure 8 Viscosity curves of various ECPs as a function of shear rate. [Color figure can be viewed in the online issue, which is available at www.interscience.wiley.com.]

increased over the entire shear rate. It is commonly known that the viscosity curves of ECPs with a higher vol % are more irregular compared to those with a lower vol %. This implies that the amount of BTO powder aggregates increased as the BTO powder contents increased. ECPs had high viscosity at a static state ($\sim 0\ s^{-1}$) and low viscosity at a high shear rate. All ECPs had a low viscosity rate of nearly 10 Pa · s at a shear rate of 100 $s^{-1}$. The viscosity of the ECP decreased as the shear rate increased, and the viscosity curve increased again along the lower curve as the shear rate increased again. The hysteresis area of the viscosity curve indicating the relative thixotropy increased as the powder content increased. The increase in the thixotropy with the powder content is because of the van der Waals force among the particles. The particles form a network structure in a stand-by state and the network results in an increase in the viscosity. If shear force was applied to the pastes, the shear force would break down the network structure.[12]

## Dielectric constant

Figure 9 shows the thickness of the cured layers as a function of the powder contents. The thickness of an ECP layer increased as the powder contents increased. Although all ECPs were screen printed in identical conditions, the thicknesses of the ECPs differed. This difference in thickness is simply due to the relative amount of the solvent. ECPs with lower BTO powder content have a high volume portion of solvent. Therefore, ECPs with lower powder contents were thinner than ECPs with higher powder contents after curing.

Figure 10 shows the specific capacitance of fabricated capacitors as a function of the powder content. The specific capacitance of the ECP layers increased as the amount of powder increased. However, it reaches a maximum value at 60 vol %, and then decreases with a further powder addition. This decrease in the specific capacitance is due to the voids or pores in the ECP layers that accommodate excess powder over the theoretical maximum packing density.[13]

Based on the above results, the dielectric constants of the ECPs with powder contents were calculated. Figure 11 shows the dielectric constants of the ECPs

TABLE I
Cure Times of the ECP Resin at Various Temperatures

| Temp. (°C) | 180 | 200 | 220 | 240 | 260 |
|---|---|---|---|---|---|
| Cure time (min) | 41 | 32 | 22 | 5 | 3 |

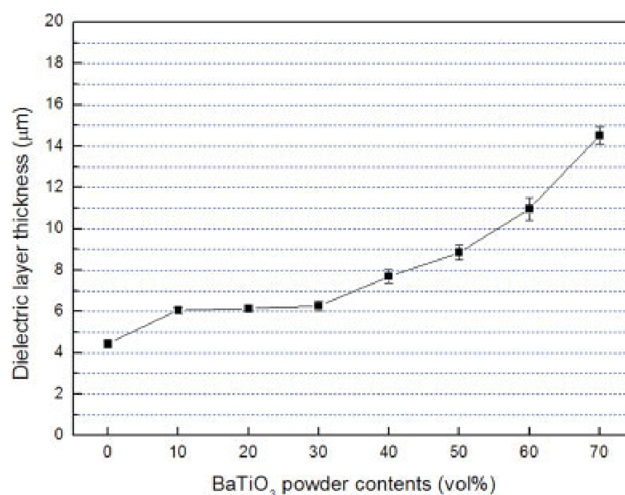


Figure 9 Thickness of the cured ECP layer as a function of BTO powder content. [Color figure can be viewed in the online issue, which is available at www.interscience.wiley.com.]

as a function of BTO powder content. The dielectric constant of the ECPs increased up to nearly 60 as the BTO powder content increased. As previously mentioned, the slow-down in the dielectric constant increment above 60 vol % occurred because the powder packing density could not reach the theoretical maximum packing density. Considering the solid content ratio, the theoretical maximum packing density is 72 vol %. However, it is exceedingly difficult to disperse powder uniformly with high-volume powder content due to the powder agglomerates and the irregular powder shape in an actual condition. As shown in Figure 12, numerous pores were observed inside the layer of 70 vol %. Therefore, it can be assumed that the actual maximum packing density is in the range of 60 to 70 vol % with single-particle packing.

The dielectric constant of BTO powder was calculated using Lichtenecker's equation. Lichtenecker's equation for polymer/ceramic composite materials is as follows:

$$\log \varepsilon_c = V_m \log \varepsilon_m + V_p \log \varepsilon_p.$$

Here, $\varepsilon_c$ denotes the dielectric constant of composite material, $\varepsilon_m$ is the dielectric constant of matrix (polymer), $\varepsilon_p$ is the dielectric constant of powder (ceramic), $V_m$ is the volume fraction of matrix (polymer), and $V_p$ is the volume fraction of powder (ceramic).

Figure 13 shows the converted dielectric constant and fitted curve. The graph was fitted going through $\varepsilon_c = 4$ at 0 BTO vol % to calculate the dielectric constant of the BTO powder. The calculated dielectric constant of the BTO powder was 424. The dielectric constant of ceramic powder varies with the particle size, and it is not easy to measure the dielectric constants of ceramic powders directly. Therefore, the dielectric constants of the ceramic powders here are obtained using an indirect method, as shown earlier.

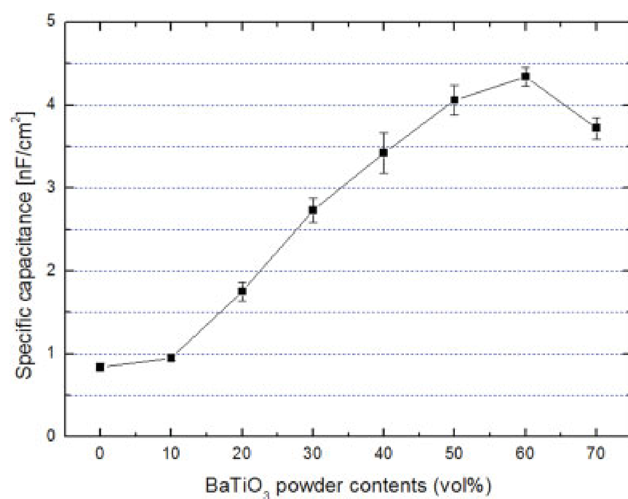


**Figure 10** Specific capacitance of the fabricated capacitors as a function of BTO powder content. [Color figure can be viewed in the online issue, which is available at www.interscience.wiley.com.]

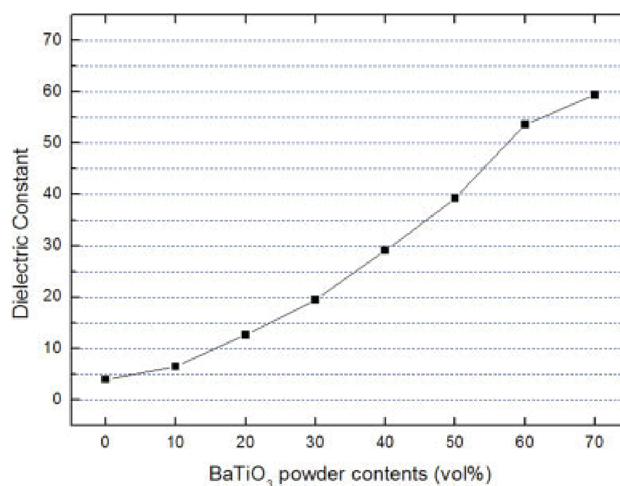


**Figure 11** Dielectric constant of the ECPs as a function of BTO powder content. [Color figure can be viewed in the online issue, which is available at www.interscience.wiley.com.]

## Reliability test result

Figure 14 shows photographic images of a fabricated embedded capacitor (a) before prepreg bonding and (b) after prepreg bonding. The ECP layers and metal pads are shown through the semitransparent FR-4 layer after prepreg bonding in Figure 14(b). Figure 15 shows the thermal cycling test result of the embedded capacitors. The capacitance of 50 vol % ECP was lower than that of 60 and 70 vol % ECP. On the other hand, the capacitances of the 60 and 70 vol % ECPs were nearly identical. This is similar to the results of the specific capacitance tests. As previously mentioned, the decrease in the capacitance is because of voids or pores in the ECP layers that accommodate excess powders over the theoretical maximum packing density.

During the thermal cycling test, dielectric losses were stable in whole cycles but the relative capacitance rapidly decreased during the initial stage. The relative capacitance stabilized around 0.9 after approximately 100 cycles due to the relaxation of the residual stress. It is widely known that the residual stress of the polymer matrix generated during the curing process can be relaxed by exposure to high temperatures above the glass transition temperature.[14] When residual stress relaxes, free volume of the polymer resin expands. Polymer chains can freely move above glass transition temperature, and the total volume appears to expand macroscopically. The increase in the free volume implies a decrease

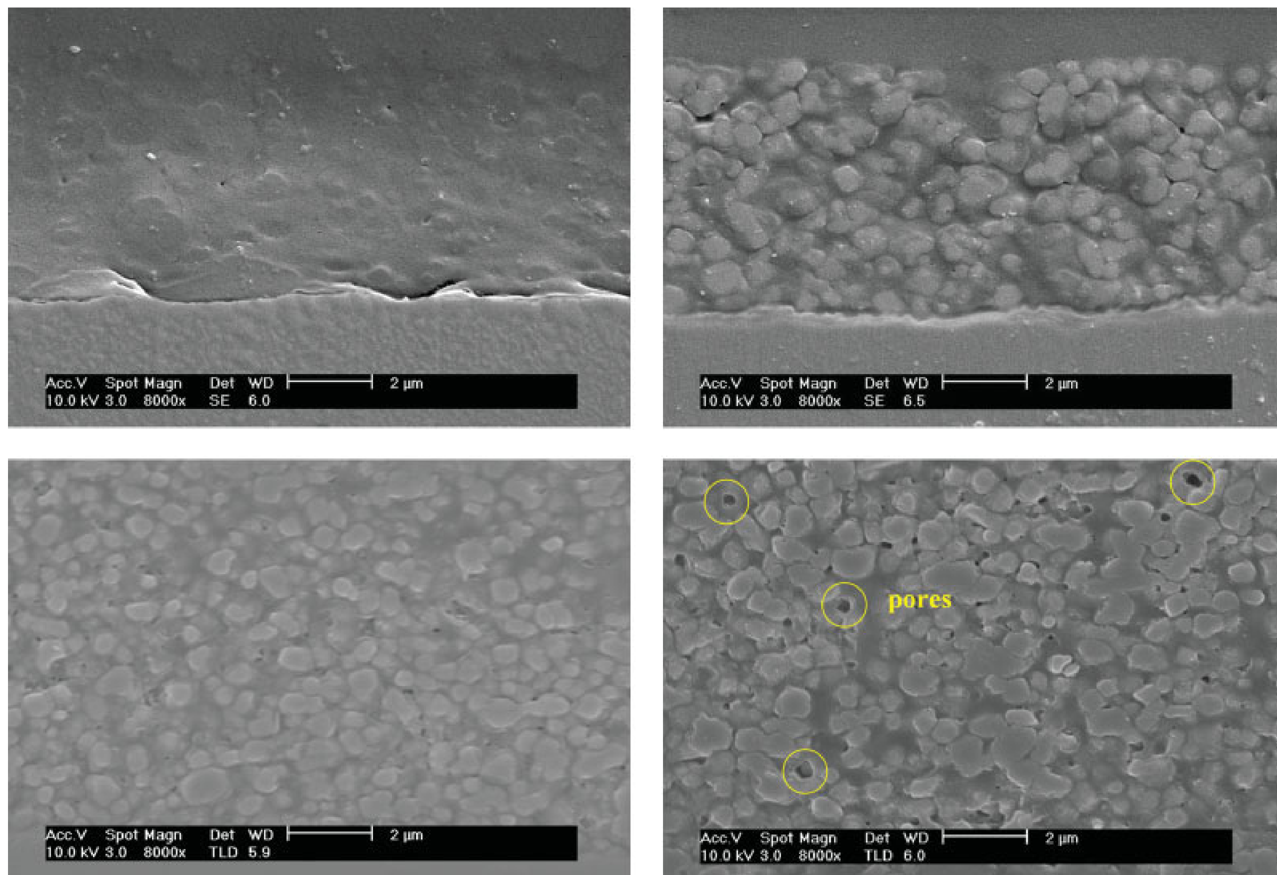


**Figure 12** Cross-sectional SEM images of (a) 0 vol %, (b) 30 vol%, (c) 60 vol %, and (d) 70 vol % ECP layers. [Color figure can be viewed in the online issue, which is available at www.interscience.wiley.com.]

in the dielectric constant, as the dielectric constant of the free volume is 1. Therefore, the overall dielectric constant of ECPs becomes lower.[15] This phenomenon is also induced by changes in the ceramic powder crystallographic structure. Capacitors made with

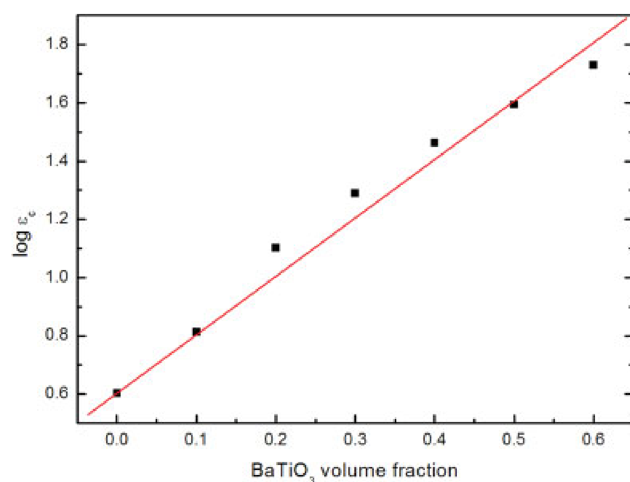


**Figure 13** Logarithm of $\varepsilon_c$ and fitted line versus the BTO volume fraction. [Color figure can be viewed in the online issue, which is available at www.interscience.wiley.com.]

ferroelectric formulations can display a decrease in the capacitance depending on the time, number of cycles, and temperature. This phenomenon, known as "dielectric fatigue" or "aging," occurs due to crystallographic changes related to the relaxation of the lattice strain energy; it does not occur with amorphous paraelectric materials.[16] One more noticeable thing in Figure 15 is that the increment of dielectric constant and decrement of dielectric loss of 70 vol % ECP was larger than those of other ECPs. It can be understood as follows. As previously mentioned, polymer resin undergoes relaxation phenomenon and decrease its dielectric constant in thermal cycles. ECP having higher volume powder contains lower volume of polymer resin. Therefore, the amount of changes in dielectric constant and dielectric loss was the smallest in 70 vol % ECP which contains the lowest volume of polymer resin among the three ECPs.

Figure 16 shows the relative capacitance and dielectric loss changes during the 85°C/85RH% test and the 100°C aging test. For the 85°C/85RH% test, both the dielectric loss and relative capacitance steadily increased. Furthermore, the increasing rates of two parameters slowed as the test time

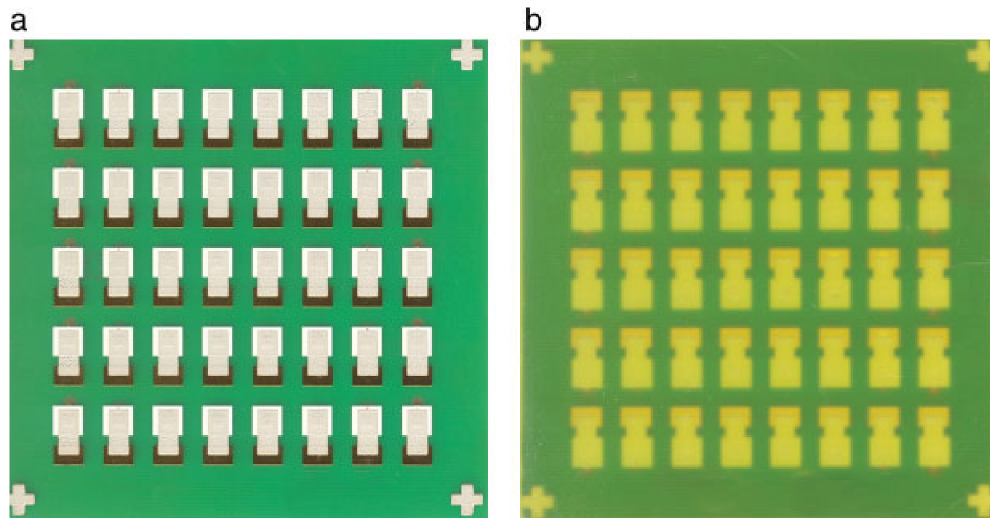


**Figure 14** Photographic images of a fabricated embedded capacitor (a) before prepreg bonding and (b) after prepreg bonding. [Color figure can be viewed in the online issue, which is available at www.interscience.wiley.com.]

progressed. It has been reported that the slow down in this rate is presumably due to the saturation of the moisture absorption level.[17,18]

As shown in Figure 16, the increment of 60 vol % ECP was larger than that of 50 vol % ECP as the polymer/ceramic interface is one of the main sites of moisture absorption. However, the increment of 70 vol % ECP was smaller than that of the 60 vol % ECP. This result can be supported as follows. An increase in loss factor and dielectric constant under the moisture uptake is a general trend in polymer materials.[19,20] It can be understood that the absorbed moisture changes the molecular dipoles. The polar group of water increases the polarity of the ECPs, resulting in an increase in the capacitance and the dielectric loss.[21,22] Experiments showed that with around 1 wt % water gain in the pure epoxy, the loss factor could increase by more than 20% whereas the dielectric constant could increase about 10%. Same trends were also observed for epoxy/ceramic composites.[23] However, changes in the dielectric

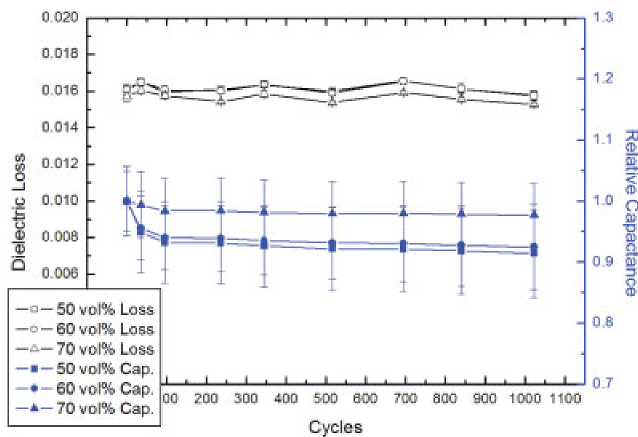


**Figure 15** Relative capacitance and dielectric loss changes during the thermal cycling test. [Color figure can be viewed in the online issue, which is available at www.interscience.wiley.com.]

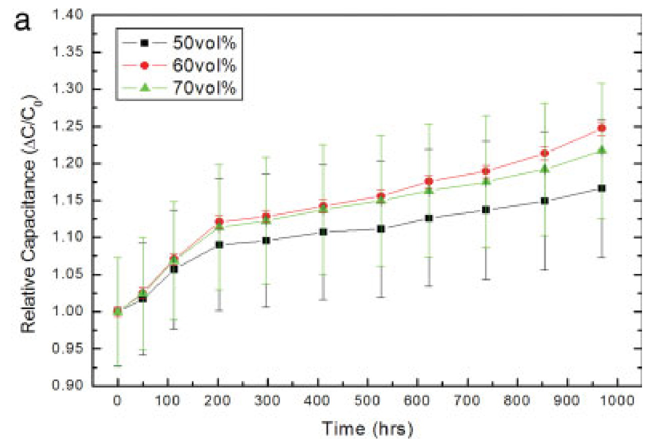


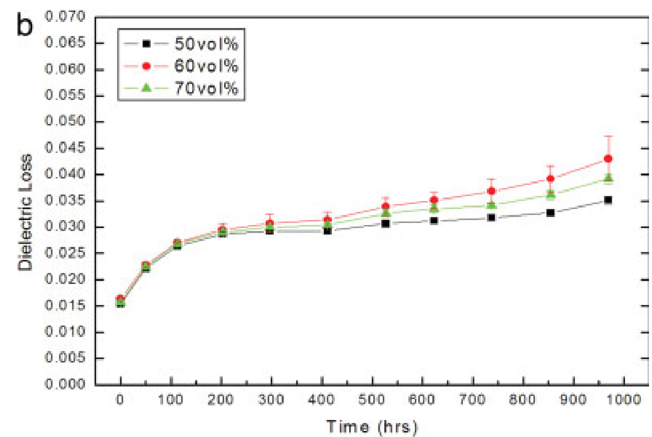


**Figure 16** (a) Relative capacitance changes and (b) dielectric loss changes during 85°C/85RH% test. [Color figure can be viewed in the online issue, which is available at www.interscience.wiley.com.]

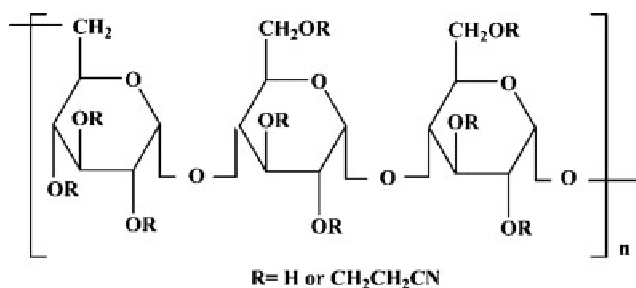


**Figure 17** Molecular structure of cyanoresin (CRS).

properties were more severe, which is usually explained by the interfacial polarization mechanism. Some authors proposed that the interphase region between the filler and epoxy matrix played an important role in determining the dielectric properties of composite materials.[24,25] One of the weakest sites against moisture in ECPs is presumably the interface between BTO powder and the resin. That is, the moisture adsorbed at the interfaces greatly affect the dielectric properties of ECPs. As previously mentioned, ECP with higher volume of BTO powder contains lower volume of epoxy resin. Also, It has larger interface area between BTO powder and the resin. However, 70 vol % ECP had many pores inside the layer. That is, it is possible that the interface area between BTO powder and the resin of 70 vol % ECP can be smaller than that of 60 vol % ECP. Therefore, the amount of moisture adsorbed at the interfaces in 70 vol % ECP can be smaller than that in 60 vol % ECP. Consequently, the result can be understood in a viewpoint of interface area between BTO powder and the resin.

### High dielectric constant polymer

The dielectric constant of a polymer/ceramic composite material can be increased by a high dielectric constant polymer. To increase the dielectric constant of the polymer/ceramic composite materials, the thermoplastic polymer in the conventional resin system was replaced by cyanoresin (CRS). Figure 17 shows the molecular structure of cyanoresin. The dielectric constant of cyanoresin is 18 and dielectric loss is 0.027 at 10 kHz. Capacitors were formed by the same screen-printing method used in the previously mentioned processes. Figure 18 shows the dielectric constant and dielectric loss of the newly formulated ECP resin, which contains 50 vol % BTO powder. Both the dielectric constant and the dielectric loss of the ECP were increased by 50%. The dielectric constant of the polymer resin calculated by Lichtenecker's equation was 8.62. This value was more than twice that of the dielectric constant of the conventional polymer resin system, 4.01. The dielectric constant of an ECP can be theoretically increased to 130 by Lichtenecker's rule when the ECP contains a maximum powder volume of 70 vol % using the newly formulated resin system.

## CONCLUSIONS

Novel screen-printable epoxy/BTO embedded capacitor pastes with high dielectric constants and good thermal stability were formulated. In terms of the material formulation, the ECPs are composed of BTO powder with a high dielectric constant, a specially formulated epoxy resin, and a latent curing agent. In terms of the fabrication process, the screen-printing method was used to fabricate a dielectric layer selectively in desired areas. The optimum curing condition of the ECP resin was determined by the curing behavior results.

For ECPs containing 70 vol % BTO powder, the dielectric constant increased to nearly 60. The theoretical maximum packing density is 72 vol %, but 60 $\sim$ 70 vol % was desirable as the actual packing density for processability. Essentially, the increment in the dielectric constant slowed down above 60 vol % due to because the voids or pores that became entrapped in the ECPs. For the material reliability tests, the embedded capacitor structure was demonstrated. Three ECPs containing 50, 60, and 70 vol % powder were selected for the tests. In the thermal cycling test, the dielectric loss was stable whereas the relative capacitance rapidly decreased at the initial stage and then stabilized at 0.9 after approximately 100 cycles. It is understood that the residual stress of a polymer matrix generated during a curing process can be relaxed by exposure to high temperatures above glass transition temperature. This phenomenon is also because of changes in the ceramic powder crystallographic structure. In the 85°C/85RH% test, both the dielectric loss and relative capacitance steadily increased. It is understood that

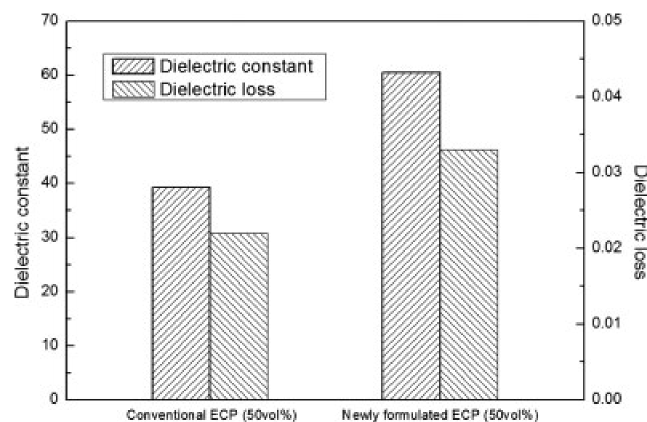


**Figure 18** Dielectric constant and dielectric loss of the newly formulated ECP compared with conventional ECPs.

the absorbed moisture affects the molecular dipole change.

The dielectric constant of the newly formulated ECP containing cyanoresin increased up to 60 with 50 powder vol %. This value was 50% higher than that using a conventional ECP. The dielectric constant of the polymer resin calculated using Lichtenecker's equation was 8.62. The dielectric constant of an ECP can be theoretically increased to 130 by Lichtenecker's rule when the ECP contains a maximum powder volume of 70 vol % using the newly formulated resin system.

## References


1. Tummala, R. R. Fundamentals of Microsystems Packaging; McGraw-Hill: New York, 2001; p 422.
2. Rector, J. In: Proc 48th Electronic Components and Technology Conference, Seatle, WA, May 1998; p 218.
3. Bhattacharya, S. K.; Tummala, R. R. J Mater Sci Mater Electron 2000, 11, 253.
4. Bhattacharya, S. K.; Tummala, R. R. Microelectron J 2001, 32, 11.
5. Rao, Y.; Ogitani, S.; Kohl, P.; Wong, C. P. J Appl Polym Sci 2002, 83, 1084.
6. Ogitani, S. IEEE Trans Adv Packing 2000, 23, 313.
7. Ramesh, S.; Huang, C.; Liang, S.; Giannelis, E. P. In: Proc 49th Electronic Components and Technology Conference, Las Vegas, NV, June 1999; p 99.
8. Cho, S.-D.; Lee, J.-Y.; Hyun, J.-G.; Paik, K.-W. Mater Sci Eng B 2004, 110, 233.
9. Potter, W. G. Epoxide Resins; ILIFFE BOOKS: London, 1970; p 65.
10. Uchino, K.; Sadanaga, E.; Hirose, T. J Am Ceramic Soc 1989, 72, 1555.
11. Arlt, G.; Henning, D.; De With, G. J Appl Phys 1985, 58, 1619.
12. Jang, K.-W.; Kwon, W.-S.; Yim, M.-J.; Paik, K.-W. IEEE Trans Compon Packing Techonol 2004, 27, 608.
13. Cho, S.-D.; Lee, S.-Y.; Hyun, J.-G.; Paik, K.-W. J Mat Sci Mater Electron 2005, 16, 77.
14. Ellis, B. Chemistry and Technology of Epoxy Resins; Chapman & Hall: London, 1993; p 104.
15. Hyun, J.-G.; Cho, S.-D.; Paik, K.-W. J Electron Mater 2005, 34, 1264.
16. Ulrich, R. K.; Schaper, L. W. Integrated Passive Component Technology; IEEE Press: New Jersey, 2003; p 84.
17. Tchangai, T.; Segui, Y.; Doukkali, K. J Appl Polym Sci 1989, 38, 305.
18. Iwasawa, T.; Ohota, K.; Sone, M. In: 12th International Conference on Conduction and Breakdown in Dielectric Liquids, Roma, Italy, July 1996, p 53.
19. Myslinski, P.; Lazowski, Z. Mater Chem Phys 1993, 33, 139.
20. Maxwell, I. D.; Pethrick, R. A. J Appl Polym Sci 1983, 28, 2363.
21. Aldrich, P. D.; Thurow, S. K.; McKennon, M. J.; Lyssy, M. E. Polymer 1987, 28, 2289.
22. Reid, J. D.; Lawrence, W. H.; Buck, R. P. J Appl Polym Sci 1986, 31, 1771.
23. Gonon, P.; Sylvestre, A.; Teysseyre, J.; Prior, C. Mater Sci Eng B 2001, 83, 158.
24. Todd, M. G.; Shi, F. G. J Appl Phys 2003, 94, 4551.
25. Todd, M. G.; Shi, F. G. Microelectronics J 2002, 33, 627.